

Liquid-infused structured surfaces with exceptional anti-biofouling performance

Alexander K. Epstein^a, Tak-Sing Wong^{a,b}, Rebecca A. Belisle^b, Emily Marie Boggs^a, and Joanna Aizenberg^{a,b,c,1}

^aSchool of Engineering and Applied Sciences, Harvard University, 29 Oxford Street, Cambridge, MA 02138; ^bWyss Institute for Biologically Inspired Engineering, 3 Blackfan Circle, Boston, MA 02115; and ^cDepartment of Chemistry and Chemical Biology, Harvard University, 12 Oxford Street, Cambridge, MA 02138

Edited by Peter G. Wolynes, Rice University, Houston, TX, and approved July 3, 2012 (received for review February 3, 2012)

Bacteria primarily exist in robust, surface-associated communities known as biofilms, ubiquitous in both natural and anthropogenic environments. Mature biofilms resist a wide range of antimicrobial treatments and pose persistent pathogenic threats. Treatment of adherent biofilm is difficult, costly, and, in medical systems such as catheters or implants, frequently impossible. At the same time, strategies for biofilm prevention based on surface chemistry treatments or surface microstructure have been found to only transiently affect initial attachment. Here we report that Slippery Liquid-Infused Porous Surfaces (SLIPS) prevent 99.6% of *Pseudomonas aeruginosa* biofilm attachment over a 7-d period, as well as *Staphylococcus aureus* (97.2%) and *Escherichia coli* (96%), under both static and physiologically realistic flow conditions. In contrast, both polytetrafluoroethylene and a range of nanostructured superhydrophobic surfaces accumulate biofilm within hours. SLIPS show approximately 35 times the reduction of attached biofilm versus best case scenario, state-of-the-art PEGylated surface, and over a far longer timeframe. We screen for and exclude as a factor cytotoxicity of the SLIPS liquid, a fluorinated oil immobilized on a structured substrate. The inability of biofilm to firmly attach to the surface and its effective removal under mild flow conditions (about 1 cm/s) are a result of the unique, nonadhesive, “slippery” character of the smooth liquid interface, which does not degrade over the experimental timeframe. We show that SLIPS-based antibiofilm surfaces are stable in submerged, extreme pH, salinity, and UV environments. They are low-cost, passive, simple to manufacture, and can be formed on arbitrary surfaces. We anticipate that our findings will enable a broad range of antibiofilm solutions in the clinical, industrial, and consumer spaces.

antifouling surfaces | biofilm resistance | slippery materials | surface engineering

Bacteria in their natural state form biofilms—structured, multicellular communities on surfaces in natural and anthropogenic environments (1, 2). Biofilms contaminate a wide variety of infrastructure elements, systems, and devices, such as plumbing, oil refineries, medical implants, food processing facilities, and heating and air conditioning networks (3–5). Marine fouling, which initiates the accumulation of bacterial biofilm on ship hulls followed by the attachment of larger marine organisms, increases the fuel burn of seafaring vessels by up to 40% (6). In medical settings, biofilms are the cause of persistent infections—implicated in 80% or more of all microbial cases—releasing harmful toxins and even obstructing indwelling catheters. Such nosocomial infections affect about 10% of all hospital patients in the United States, result in nearly 100,000 deaths annually, and consequently drive much of current biotechnology research (7–9).

Biofilms protect their constituent cells in various ways, which makes both clinical and industrial contamination difficult and/or costly to treat. As self-organized communities, biofilms have evolved as differentiated cell phenotypes performing complementary functions. The cooperative behavior of bacterial cells, mediated by cell–cell communication and other factors, enables an increased metabolic diversity and efficiency as well as an

enhanced resistance to environmental stresses, antimicrobial agents, and immune response. For example, some constituent cells are active in spreading the biofilm while others enter dormant states invulnerable to many antimicrobials (10–13). The macroscopic physical properties of biofilms, in which cells are bound together by a protein and exopolysaccharide matrix, also protect them by resisting penetration of conventional liquid and vapor-phase antimicrobials (14). Indeed, the resistance to threats covers a wide range of treatments. For example, exposure to chlorine bleach for 60 min still leaves live cells (8); biofilms in pipes flushed continuously with multiple biocides over 7 d recolonize the pipes (15), and biofilms can survive in bottled iodine solution for up to 15 months (16).

Clearly, it is extremely desirable to prevent rather than treat biofilm formation, and accordingly, a wide range of bacteria-resistant surfaces have been proposed. Most strategies rely either on a release of biocidal compounds or on inhibiting adhesion (17–20). In the first case, techniques involve the design of coatings or bulk materials that release agents such as antibiotics, quaternary ammonium salts, and silver ions into the surrounding aqueous environment (19). The latter approach has focused on the use of surface chemical functional groups that inhibit protein adsorption as a means to inhibit bacterial adhesion. Examples include low-surface-energy, weakly polarizable materials (e.g., Teflon) that minimize van der Waals interactions (21); zwitterionic, mixed-charge, or amphiphilic materials (22) that utilize surface inhomogeneities (e.g., charge and hydrophobicity) to frustrate adhesion at the nano to micrometer scales (23); and hydrophilic polymeric materials that form highly hydrated surfaces to inhibit protein adhesion (24). One of the most commonly studied hydrophilic modifications is poly(ethylene glycol), or PEG (25, 26). Solid/liquid/liquid antifouling interfaces based on complex coacervation and/or complex coacervate core micelles have also been reported (27–29). More recently, structured superhydrophobic surfaces mimicking the Lotus leaf have been suggested (17, 30).

Each of these strategies, however, is generally transient. Materials that persistently resist bacteria are difficult to achieve by surface chemistry or surface structuring alone. The surface molecules are subject to desorption over time, a limitation that has driven much research in the area of strengthening the physisorption of, for example, PEG coatings (19). However, even if no desorption occurs and bacteria are unable to attach directly to a substrate, nonspecific adsorption of proteins and surfactants secreted by bacteria can still mask the underlying chemical func-

Author contributions: J.A., A.K.E. and T.S.W. designed research; A.K.E., T.S.W., E.M.B. and R.A.B. performed research; A.K.E., T.S.W., R.A.B. and J.A. analyzed data; and A.K.E., T.S.W. and J.A. wrote the paper.

The authors declare no conflict of interest.

This article is a PNAS Direct Submission.

Freely available online through the PNAS open access option.

¹To whom correspondence should be addressed. E-mail: jaiz@seas.harvard.edu.

This article contains supporting information online at www.pnas.org/lookup/suppl/doi:10.1073/pnas.1201973109/-DCSupplemental.

tonality (31–33). Additionally, any defects in the surface chemistry could serve as nucleation sites for bacterial attachment. Structured superhydrophobic surfaces in the Cassie (trapped air) state are prone to irreversible wetting (Wenzel transition), especially with the production of bacterial surfactant, seriously limiting their lifetime in submerged environments (34). Strategies involving leaching of biocides are limited over a longer timescale because their reservoir is finite and subject to depletion (20). Also, the emergence of antibiotic- and silver-resistant pathogenic strains, along with new restrictions on the use of biocide-releasing coatings in the marine environment, has necessitated the development of new solutions (35–37).

Traditional antibiofouling surfaces are fundamentally in solid forms (i.e., their surface atoms/molecules are static or quasi-static in nature). Therefore, permanent interactions between the solid surfaces and the biological adhesives can eventually be established depending on the time scales of the adhesion processes, which then lead to stable attachment and biofouling. Creating a surface that possesses dynamic features down to the nanometer scale, i.e., mobility of surface molecules or structures, may inhibit these permanent interactions, thereby significantly disrupting the biological adhesion. A potential approach to generating dynamic surfaces is to utilize a stabilized liquid interface. Inspired by the *Nepenthes* pitcher plant (38), we recently developed a new model of omni-repellent surface, one based not on an unstable and transient solid-air Cassie-type interface, but rather on a stable, immobilized, and smooth liquid surface locked in place by a specially designed porous solid, allowing the material to function even when submerged (39). This novel slippery liquid-infused porous surface (SLIPS) is a material concept that exploits the extreme stability of the fully wetted liquid film to maintain repellency across a broad range of temperature, pressure, surface tension, and other conditions (39). Specifically, stable SLIPS is designed based on three important criteria: (i) the chemical affinity between the lubricating fluid and the solid should be higher than that between the ambient fluid and the solid; (ii) the solid should preferably be roughened so as to increase the surface area for the adhesion of the lubricating fluid and its immobilization;

and (iii) the lubricating fluid and the ambient fluid must be largely immiscible. Based on these principles and following a set of surface energy parameters (39), any porous or nanostructured solid—as long as it can be roughened by surface deposition and/or etching techniques such as lithographic structuring, epitaxial growth of nanostructures, sand blasting, spraying, colloidal assembly, electrospinning, sol-gel process etc., followed by surface functionalization to match the chemical nature of the infiltrated lubricant chosen to be immiscible with the ambient fluid—can form a stably immobilized slippery interface (Fig. 1A).

Here, we report on the exceptional ability of SLIPS to prevent biofilm attachment. The SLIPS liquid in our setup is infiltrated into a porous polytetrafluoroethylene (PTFE) substrate (40–43) or microstructured fluoro-silanized Si wafer and presented as a smooth liquid–liquid interface to bacteria. Through rigorous quantification, we demonstrate that our SLIPS platform prevents up to 96–99% of common bacterial biofilms from attaching over at least a 7-d period in a low flow environment, a 35 times greater advance over best-case-scenario, state-of-the-art surface chemistry treatments based on PEGylation (44). This result extends across bacterial species, including the clinical pathogens *P. aeruginosa*, *S. aureus*, and *E. coli*. We furthermore confirm that the lack of biofilm attachment is not caused by any cytotoxicity of the SLIPS liquid, but by its exceptional mobility on the slippery interface. Moreover, the SLIPS antibiofilm surfaces are stable when submerged, under extreme pH, salinity and UV exposure conditions, and can be formed on arbitrarily shaped surface contours, such as catheters, pipelines, or other systems requiring prolonged biofilm resistance.

Results and Discussion

In a simple test scheme, *Pseudomonas aeruginosa* TB culture was deposited in puddles that were statically incubated on three surface typologies: (i) a porous PTFE membrane (0.2 μm pore size) served as a conventional low-adhesive, superhydrophobic control surface; (ii) a PTFE membrane infused with perfluoropolyether (Krytox-103) formed a SLIPS material (Fig. 1B–E); (iii) and a fluoro-silanized patterned silicon wafer featuring four different high-aspect-ratio micropost arrays presented a superhydrophobic

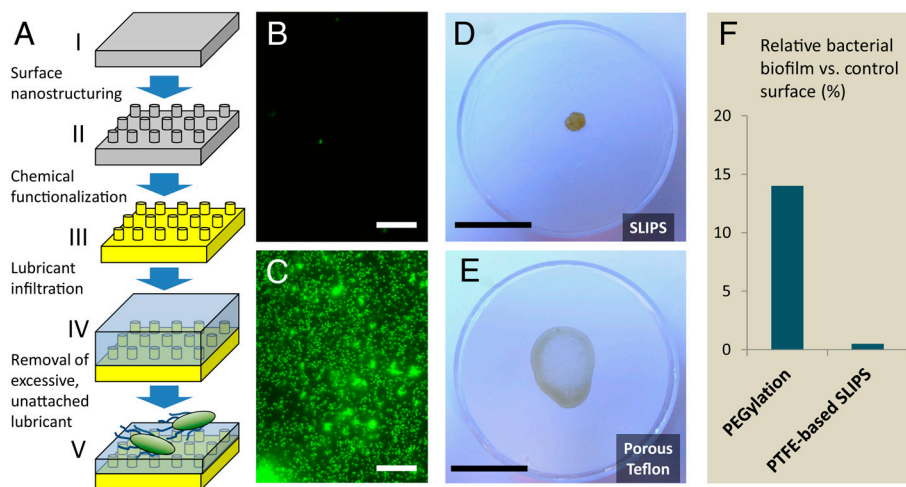


Fig. 1. SLIPS preparation and biofilm attachment to the surfaces investigated in this study. (A) Schematic of slippery liquid-infused porous surface (SLIPS) material concept. A flat substrate (i) is nano-patterned or roughened (ii), chemically functionalized (iii), and infused with a compatible lubricating liquid (iv), of which the excess is removed (v). Porous Teflon substrates used in this study are stage III-ready for the infiltration with perfluorinated lubricants. The two-part system presents a “slippery” surface of highly immiscible immobilized liquid to bacteria. (B–C) Fluorescence micrographs of attached bacteria following 48 h incubation of *P. aeruginosa* biofilm on SLIPS (B) and superhydrophobic PTFE (C). Scale bar = 30 μm. (D–E) Remains of an evaporated drop of *P. aeruginosa* biofilm-forming culture on SLIPS (D) and superhydrophobic PTFE (E). The poorly attached biofilm on the SLIPS substrate cleanly retracts from the surface as it evaporates (see [Movie S3](#)), leaving behind a small, easily removable pellet (see [Movie S4](#)). In contrast, biofilm grown on the PTFE and microstructured superhydrophobic silicon ([Movie S1](#)) shows complete wetting of the surface and leaves behind a slimy, firmly attached coffee ring. Scale bar = 2 cm. (F) Comparison of biofilm attachment to our SLIPS substrate after 7 d and to a PEGylated substrate after 5 h, as reported in (44). Even assuming a best-case scenario in which its 5 h PEG performance can be maintained at 7 d without desorption or masking of surface chemistry, the 0.4% relative attachment to SLIPS represents a >30 times improvement.

surface, able to repel and roll off water (Fig. S1 and Movie S1). The use of PTFE membrane in combination with perfluorinated lubricant has the advantage of avoiding the first two steps in the SLIPS fabrication scheme shown in Fig. 1A. After 48 h of room temperature growth in static culture, the viable cell concentration of the imposed bacterial cultures on both surfaces was on the order of 10^8 mL⁻¹. The bacteria were fixed and stained, and the fluorescence micrographs of resulting growth are shown in Fig. 1B–C. While robust and uniform biofilm coverage is observed on both flat PTFE and superhydrophobic silicon, only sparse and isolated cells are seen on the SLIPS. In fact, early-stage bacterial growth on PTFE and SLIPS submerged in static culture (Fig. S2) produces a submonolayer of unattached cells on SLIPS that randomly drift with convective currents in the liquid. The test surfaces were also manually tilted to compare the adhesion of the macroscopic biofilm slime as shown in Fig. 2 and Fig. S1 and Movies S1 and S2. A droplet of bacterial medium grown on the control and superhydrophobic substrates shows complete wetting of the surface and either leaves a film of firmly attached slime or remains pinned at the ingrown biofilm as it is tilted. In contrast, biofilm on the SLIPS substrate (Fig. 2 and Movie S2) slides readily upon simple tilting without leaving any visible residue.

We further analyzed the contact line pinning characteristics of the SLIPS and porous Teflon surfaces by monitoring the evaporation dynamics of bacterial culture droplets (Fig. S3 and Movie S3) as well as the stains remaining on the surfaces upon drying (Fig. 1D–E, Fig. S4 and Movie S4). In the absence of pinning, the droplet should follow a nearly constant contact angle mode of evaporation (45), without the formation of a coffee ring stain (46). Indeed, this mode was consistent with our observations (Fig. S3 and Movie S3) of the contact line movement for the bacterial droplet evaporation from the SLIPS surface. The absence of the coffee ring formation also indicates that the adhesion of the bacteria on the SLIPS is small as compared to the forces imparted by the meniscus of the droplet (47, 48), and we demonstrate in Fig. S4 and Movie S4 that the dried biofilm is extremely easily removed from SLIPS by adhesive tape. In contrast, an evaporating droplet on the porous Teflon was strongly pinned, leading to a constant contact area mode of evaporation (45) and to the formation of an irremovable coffee ring (46). These visual demonstrations of biofilm nonattachment to SLIPS and of resisting 3.5×10^8 mL⁻¹ bacterial liquid are consistent with both macroscopic and microscopic quantification in the present study.

While the above static experiments clearly show poor biofilm attachment to SLIPS compared to other surfaces, it is important to emphasize that many, if not most, environments in which biofilm prevention is imperative are not static. Most submerged biofilm formation occurs under various flow conditions (e.g., in plumbing, ship hulls, catheters, or implant surfaces), and biofilms are known to attach robustly to substrates under flow (49, 50).

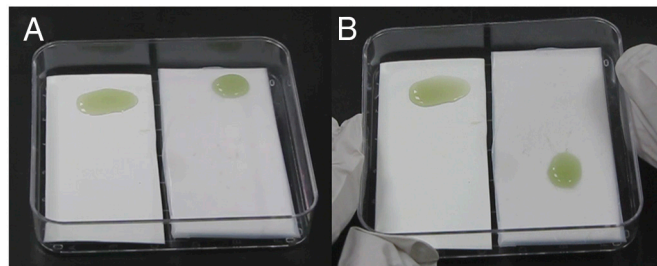


Fig. 2. *P. aeruginosa* biofilm puddles grown for 24 h on a PTFE porous surface and a PTFE SLIPS surface infused with Krytox 103, before (A) and after (B) being tilted to test biofilm adhesion. A robust, ingrown, and therefore pinned biofilm forms on the control PTFE substrate, whereas biofilm on the SLIPS substrate slides readily without leaving any slime film or other visible residue (see Movie S2).

The design of surfaces on which biofilm attachment is sufficiently weak such that the cells can be removed even by gentle flow would provide a persistent antifouling strategy superior to bactericidal or chemical approaches. Accordingly, biofilm attachment was studied on test surfaces lining a dual flow cell, through which the bacterial culture was continuously circulated by a peristaltic pump. Under flow conditions of 10 mL/min volumetric flow rate and approximately 1 cm/s linear velocity, both a control PTFE and SLIPS surface were exposed in parallel to PA14 bacterial culture for 24 h, 48 h, and 7 d (168 h) periods. We further verified that the functionality of SLIPS does not degrade over the experimental time frame (Fig. S5). Indeed, the PTFE and SLIPS substrates following 48 h growth show a yellowish, slimy appearance for control substrate and a visually uncontaminated SLIPS (Fig. 3A and B). To quantitatively compare the biomass accumulated in flow by optical density, equal-area samples of the substrates with attached biofilm were stained by crystal violet (51). This macroscopic assay showed a dramatic difference between the substrates, seen in Fig. 3A and B. Crystal violet absorbance, proportional to the attached biomass, showed a 99.6% average reduction in biofilm on SLIPS as compared to control PTFE following 7-d bacterial growth in the flow (Fig. 3C). By comparison, PEGylated titanium surfaces have been reported to reduce biofilm attachment by 86% after 5 h of growth (44), and massive biofilm growth occurs after that period. We measured the 48 h growth of *P. aeruginosa* on Ti-coated glass slides [prepared as described in (44)] to differ by <19% from PTFE, indicating similar long-term biofilm attachment on these two controls and thus a similar starting point for attachment reduction. Even if no PEG desorption or chemical masking were to occur following 7 d in bacterial culture, the 14% relative biofilm attachment (44) would still be approximately 35 times more than we measured on the SLIPS substrate after one week of growth (Fig. 1F).

It should be noted that the flow velocity of approximately 1 cm/s that we chose for our study was intended as a conservatively gentle condition. In other environments where biofilms form (e.g., a residential building water pipe or a ship hull), typical flow velocities can be on the order of 1 m/s and 10 m/s respectively, with proportionately higher shear forces that would accelerate biofilm removal from a SLIPS substrate. In biological and biomedical systems such as indwelling catheters, urinary tracts, and the human vascular system, flow velocities can also be more

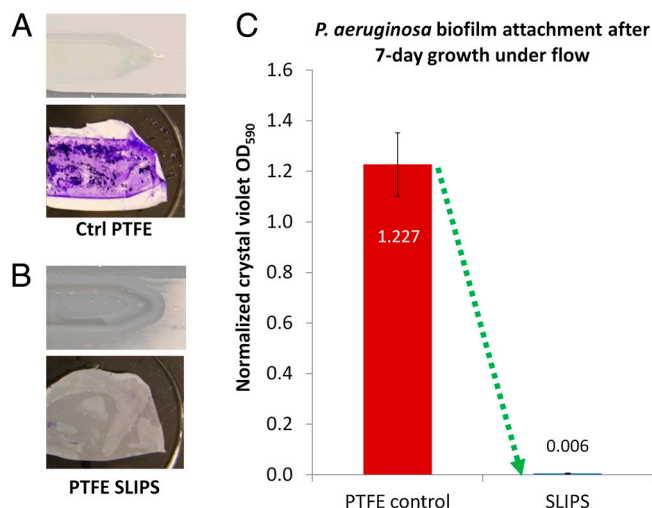


Fig. 3. Characterization of biofilm attachment to SLIPS and PTFE in a dual-chamber flow cell with 10 mL/min flow rate. (A–B) Photographs of the control PTFE and SLIPS substrates after the flow cell was opened following 48 h growth, both before (Top) and after (Bottom) crystal violet staining. (C) Crystal violet staining-based quantification of accumulated biomass on SLIPS versus control PTFE following 7 d of growth.

aggressive, on the order of 10–100 cm/s, although 1–10 cm/s is more typical (52, 53). In addition to flow, we further examined the robustness of slippery behavior of SLIPS against extreme environmental conditions: 7 d immersion in concentrated brine (10 times the salinity of ocean water), in acid (pH approximately 1) and base (pH approximately 14), as well as exposure to 1000 kJ/m² of UV, which is approximately the annual UV exposure in the southwestern United States. As shown in Fig. S6 and Movies S5 and S6, the slipperiness of the interface did not degrade over our experimental time frame.

To characterize biofilm attachment to PTFE and SLIPS substrates on the microscale, we fluorescently imaged multiple sample areas following 24 h, 48 h, and 7 d flow condition growths. Biofilm on the control surface appeared characteristically dense, three-dimensional, and uniform (Fig. 4 A and B). On the SLIPS, only sparse, isolated single cells or microcolonies were observed (Fig. 4 C and D), and these appeared to be unattached or poorly attached; i.e., drifting with convective currents in the ambient fluid. The average fluorescence intensities of 20 representative fields of view per substrate were computed as numeric pixel averages [(R + G + B)/3]. While not fully capturing intensity from out-of-focus biofilm structure on the control surface, the control values may be considered a lower limit; thus there is at least a 98% average intensity reduction in the fluorescence signal from PTFE to SLIPS, similar to the global quantification by crystal violet absorbance.

To confirm that the dramatic biofilm attachment inhibition on SLIPS substrates is not a result of cytotoxicity of the SLIPS liquids, we screened four of the lubricants for effects on bacterial growth. These included the Krytox 103, Krytox 100, perfluorotriptylamine (FC70), and perfluorodecalin (54). The growth curves of *P. aeruginosa* were measured following growth in shaken TB cultures, thereby assuring uniform exposure, with 1% concentrations of each SLIPS liquid. As seen in Fig. 4E, statistically indistinguishable bacterial growth occurred at 3, 6, 9, and 30 h for all tested SLIPS liquids as compared to the control culture with no lubricant. Equivalent or lower concentrations of three negative controls—silver nitrate (a common antiseptic compound and representative of silver impregnated surfaces), bleach, and glutaraldehyde (commonly used for clinical tool sterilization)—were also investigated. As expected, all three exhibited massive toxicity, in contrast to the null effect of the SLIPS liquids.

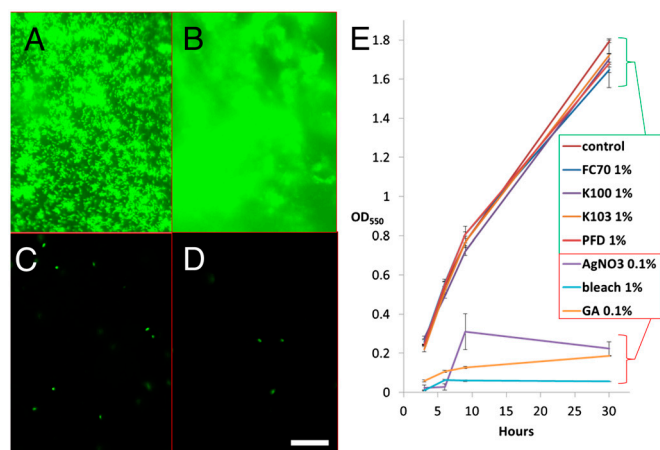


Fig. 4. (A–D) Fluorescence imaging of *P. aeruginosa* biofilm attachment on control PTFE (A, B) and SLIPS (C, D) surfaces after 24 h (A, C) and 7 d (B, D) growths in 10 mL/min flow. Scale bar = 30 μm. (E) Indistinguishable growth curves [$n = 3$] of *P. aeruginosa* cultured in shaken TB media containing 1% of the SLIPS liquids FC70, Krytox 100, Krytox 103, and perfluorodecalin at 3, 6, 9, and 30 h suggests no toxicity and biocompatibility of the lubricant, while silver nitrate, bleach, and glutaraldehyde exhibited massive toxicity within these timeframes.

The exceptional ability of SLIPS to resist the attachment of *P. aeruginosa* by providing a nonadhesive, slippery interface, independent of any specific chemical or physical features of the cells, coupled with the stability of the SLIPS in diverse, including submerged, environments, raised the exciting question of SLIPS's potential as a general antifouling material resisting a broad spectrum of biofilms. Of particular importance is the ability to combat pathogenic biofilms encountered in biomedical settings and accumulated on devices such as catheters and implants under flow. To test the species generality of the SLIPS platform, we studied attachment of two other clinically important biofilm-forming pathogens, *Staphylococcus aureus* (SC01) and *Escherichia coli* (ZK2686), for 48 h under identical flow conditions. As shown in Fig. 5 A and B, *S. aureus* attachment was reduced by 97.2% and *E. coli* by 96% versus PTFE, based on crystal violet absorbance. While these species form variably robust biofilms on PTFE, their final attachment to SLIPS was all comparably minimal. Visualized by fluorescence in Fig. 5 C–F, dense, uniform bacterial coverage and sparse, isolated cells were observed on the control surface and SLIPS, respectively. This indicates that SLIPS's anti-fouling function is nonspecific and spans phylogenetically diverse pathogenic biofilm-forming bacteria.

From our experimental observations, it is apparent that the bacteria are presented with a smooth liquid “surface,” and as such, there may be no ability to anchor to the mobile interface via pili and other cellular mechanisms as would be possible on a solid surface (55, 56). The SLIPS liquid is also immiscible with aqueous bacterial medium; the surface tension at the interface (56.0 ± 0.9 mN/m) (39) may be difficult for bacteria to penetrate, even with bacterial surfactant production. Indeed, we did not observe bacteria embedding within the SLIPS, indicating that bacteria cannot swim through the interface. This is consistent with reported confinement of bacteria, biofilms and even mammalian cells in oil-water emulsion studies (57–61). Interestingly, whereas *S. aureus* is reported to adhere well to a hexadecane-water interface (approximately 45 mN/m), and whereas *P. aeruginosa* is a known hydrocarbon degrader (62), neither attaches to form biofilm on the immobilized perfluorinated fluid in our SLIPS. Whether any cohesive biofilm does transiently form on SLIPS before being sheared off by even mild flow, or whether the bacteria simply remain planktonic in the medium, remains an interesting question. Without access to the solid material beneath a SLIPS liquid, bacteria may be unable to attach, remaining subject to ambient flow and thus subject to passive removal.

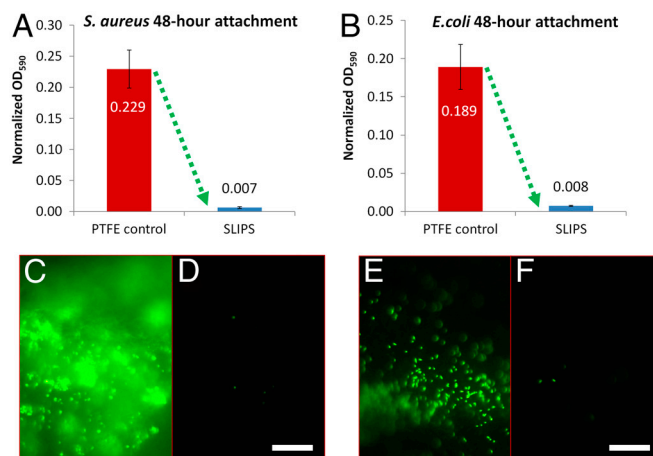


Fig. 5. Biofilm attachment reduction by SLIPS extends to other highly pathogenic bacteria species. (A–B) Comparison of the attachment of biofilm-forming *Staphylococcus aureus* (A) and *Escherichia coli* (B) to PTFE and SLIPS. (C–F) Fluorescence imaging of *S. aureus* (C–D) and *E. coli* (E–F) bacterial cells attached to the control (C, E) and SLIPS (D, F) substrates, respectively. Scale bar = 30 μm.

Given the vast diversity of bacteria and their motility and adhesive approaches, it would be an interesting future study to consider their mobility across liquid-liquid interfaces as a function of varying interfacial tension and other factors.

In any case, at present there are no known nontoxic antibiofilm synthetic surfaces that are capable of preventing diverse biofilm accumulation over a period of 1 wk or longer under low flow conditions. Our result of up to 96–99.6% reduction in attachment over a 7-d range is a step change beyond state-of-the-art technology and is promising for a wide range of applications.

Conclusion

We have demonstrated a novel approach for preventing surface biofilm attachment, simply presenting a structured surface with immobilized liquid to bacteria, and obviating the need for biofilm control by toxic release, intensive chemical attack, or even mechanical removal. We have presented proof of concept, including a 1–2 order of magnitude advance in 7-d attachment prevention versus best-case-scenario PEG-functionalized surfaces, for one of the most common and opportunistic pathogens in both terrestrial and aquatic environments, *Pseudomonas aeruginosa*, as well as for *Staphylococcus aureus* and *Escherichia coli*. From a fabrication standpoint, the SLIPS lubricant can be chosen from a wide range of biocompatible liquids, while the immobilizing texture of the solid substrate can be derived by simply casting, growing or etching porous texture directly on material surfaces that must remain biofilm-free. For example, a variety of methods to roughen and modify solid substrates of arbitrary geometries, including pipes, have been developed (63–65), all of which could be converted into SLIPS upon appropriate surface functionalization and addition of a lubricant. Insensitive to the structural details of the underlying porous solid (39), stable when submerged, and showing no degradation under a range of diverse environmental conditions, integrated SLIPS-based surfaces that are both nontoxic and biofilm-resistant hold exciting promise for a range of cost- and potentially life-saving antifouling applications in the biomedical and industrial spaces.

Methods

SLIPS Fabrication. To prepare SLIPS, lubricating fluid was added onto the porous solids to form an over-coated layer. The lubricating fluids used for the antibiofilm experiments were perfluorinated fluids: perfluoropolyethers (Dupont™ Krytox® 100 and 103), perfluorotripropylamine (3M™ Fluorinert™ FC-70), and perfluorodecalin (Sigma Aldrich). The porous solids used were Teflon membranes with average pore size of ≥ 200 nm and thickness of approximately 60–80 μm , which were manufactured by Sterilitex Corporation, WA, and were used without further modification. With matching surface chemistry and substrate roughness, the lubricant spreads spontaneously onto the whole substrate through capillary wicking. The excess liquid not bound to the underlying solid was removed by tilting the surface and mildly applying compressed air.

Silicon Microstructure Array Fabrication. Superhydrophobic microstructure arrays were fabricated on a 4" silicon wafer by the Bosch process (66). The microstructures consist of four types of geometries: $d = 500$ nm high-aspect-ratio (HAR) nanoposts, with pitch $p = 2 \mu\text{m}$; $d = 1 \mu\text{m}$ HAR microposts, $p = 3 \mu\text{m}$; 5 μm T-shaped microposts; and 10 μm T-shaped microposts that were rendered hydrophobic by exposing to a heptadecafluoro-1,1,2,2-tetrahydrodecyltrichlorosilane (Gelest Inc.) vapor.

SLIPS Stability Characterization. The robustness of SLIPS in extreme environments was tested by immersing samples for 7 d in acid (concentrated hydrochloric acid, 37%, pH approximately 1), base (concentrated potassium

hydroxide, 47%, pH approximately 14), concentrated brine (sodium chloride solution, approximately 335.7 g/L) equivalent to 10 times oceanic salinity, and by exposing to 50 mW/cm² of broadband UVA radiation for 33 min (equivalent to annual ambient UV exposure of 1000 kJ/m²). Slipperiness was quantified for each test by recording the sliding angle of a 30- μL water droplet (as well as an octane droplet) applied to the surface in air, using a Fowler Premium V-block variable-angle stage. The water droplets were applied at 0° (horizontal) and the angle was slowly adjusted in 0.5° increments until droplet movement was observed.

Bacterial Preparation and Growth. Bacterial strains *Pseudomonas aeruginosa* PA14, *Staphylococcus aureus* SC01, and *Escherichia coli* ZK2686 were each grown in LB medium (EMD LB Broth Miller) overnight at 37 °C in loosely capped tubes on an orbital shaker to the stationary phase. This LB preculture was then seeded at 1% concentration in one of the following: TB growth medium (BD Bacto Tryptone) for *P. aeruginosa*; TSB medium supplemented with 0.5% glucose and 3% NaCl for *S. aureus*; or M9 medium for *E. coli*. These bacterial cultures were incubated on the bench at room temperature.

Flow Cell Setup. A Tygon tube of inner diameter 3 mm was mounted in a peristaltic pump (Cole Parmer) and connected to a dual-chamber 3D-printed flow cell (chamber dimensions $l = 10$ cm, $w = 1$ cm, $h = 1$ mm). The bottom surface and sidewalls of each chamber were lined with press-fit porous Teflon membrane; one was infused with Krytox 103 to create a SLIPS and the other was left untreated as a control. Bacterial culture was pumped into each tube until the loop was full and trapped air had been eliminated, after which the pump was operated for the desired periods of time (24 h, 48 h, 7 d).

Toxicity Screening. Shaken cultures of 1% *P. aeruginosa* in TB were grown in triplicate in the presence of 1% by volume of the following reagents: Krytox 100, Krytox 103, Perfluorodecalin, FC70, bleach, as well as with 0.1% of AgNO₃, and 0.1% glutaraldehyde. Background samples containing only media and reagents were also prepared, as well as control cultures without added reagents. Samples were incubated in an orbital shaker at 37 °C at 200 rpm. Optical density measurements at 550 nm were taken at 3, 6, 9, and 30 h on a Perkin Elmer Lambda 40 UV-Vis spectrometer. Optical densities were normalized by subtracting backgrounds, i.e., the reagents in TB only.

Imaging and Analysis. For fluorescence imaging of attached bacterial cells, the substrates were removed, gently rinsed in phosphate-buffered saline (PBS) (Lonza Biowhittaker), and the adherent bacteria were fixed by 5% glutaraldehyde solution for at least 1 h. 0.01% Triton X100 in PBS (PBST) was used to permeabilize the bacteria membranes over 15 min, after which the cells were stained with 0.5 μM SYTOX green nucleic acid stain (Invitrogen) in PBST for 30 min. Imaging was performed on a Leica DMX microscope. To analyze the fluorescence intensity of the micrographs, the average intensity image of each sample's micrograph set was generated in ImageJ and the average $[(R + G + B)/3]$ pixel value and standard deviation were computed for each average intensity image.

Biofilm Quantification by Crystal Violet Staining. PTFE substrates were carefully sectioned with a scalpel into 3×3 cm segments, removed from the flow cell, gently rinsed in PBS, and stained by 0.1% crystal violet for 20 min. The stained samples were rinsed in a DIW bath and the bound crystal violet was eluted from each sample into 4 mL of 100% EtOH. Absorbance values at 590 nm of the resulting EtOH solutions were measured on a Perkin Elmer Lambda 40 UV-Vis spectrometer.

ACKNOWLEDGMENTS. We thank Allon Hochbaum for helpful discussion on toxicity and manuscript advice, Ben Hatton and James Weaver for supplying the peristaltic pump and the flow cell, Ilana Kolodkin-Gal for microbiological advice and materials, and Meredith Duffy for additional assistance. TSW thanks Croucher Foundation Postdoctoral Fellowship for financial support. The work was partially supported by the Wyss Institute for Biologically Inspired Engineering at Harvard University and ONR under the award N00014-11-1-0641.

- Shapiro J (1998) Thinking about bacterial populations as multicellular organisms. *Annu Rev Microbiol* 52:81–104.
- Wilking JN, Angelini TE, Semnara A, Brenner MP, Weitz DA (2011) Biofilms as complex fluids. *MRS Bull* 36:385–391.
- Costerton JW, Stewart PS (2001) Battling biofilms—The war is against bacterial colonies that cause some of the most tenacious infections known. The weapon is knowledge of the enemy's communication system. *Sci Am* 285:74–81.
- Kumar CG, Anand S (1998) Significance of microbial biofilms in food industry: A review. *Int J Food Microbiol* 42:9–27.
- Chmielewski R, Frank J (2003) Biofilm formation and control in food processing facilities. *Compr Rev Food Sci F* 2:22–32.
- Dalley AACaR (1987) Barnacle fouling and its prevention. *Barnacle Biology*, ed AJ Southward (A.A. Balkema, Rotterdam, NL), pp 419–433.
- Schachter B (2003) Slimy business—The biotechnology of biofilms. *Nat Biotechnol* 21:361–365.

8. Davies D (2003) Understanding biofilm resistance to antibacterial agents. *Nat Rev Drug Discov* 2:114–122.
9. Klevens R, et al. (2007) Estimating health care-associated infections and deaths in US hospitals, 2002. *Public Health Rep* 122:160–166.
10. Ben-Jacob E, Cohen I, Gutnick DL (1998) Cooperative organization of bacterial colonies: From genotype to morphotype. *Annu Rev Microbiol* 52:779–806.
11. Klausen M, Aaes Jørgensen A, Molin S, Tolker Nielsen T (2003) Involvement of bacterial migration in the development of complex multicellular structures in *Pseudomonas aeruginosa* biofilms. *Mol Microbiol* 50:61–68.
12. Stewart PS, Franklin MJ (2008) Physiological heterogeneity in biofilms. *Nat Rev Microbiol* 6:199–210.
13. Vlamakis H, Aguilar C, Losick R, Kolter R (2008) Control of cell fate by the formation of an architecturally complex bacterial community. *Gene Dev* 22:945–953.
14. Epstein A, Pokroy B, Seminara A, Aizenberg J (2010) Bacterial biofilm shows persistent resistance to liquid wetting and gas penetration. *Proc Natl Acad Sci USA* 108:995–1000.
15. Anderson RL, Holland BW, Carr JK, Bond WW, Favero MS (1990) Effect of disinfectants on pseudomonads colonized on the interior surface of PVC pipes. *Am J Public Health* 80:17–21.
16. Panlilio AL, et al. (1992) Infections and pseudo-infections due to povidone-iodine solution contaminated with *Pseudomonas cepacia*. *Clin Infect Dis* 14:1078–1083.
17. Genzer J, Efimenko K (2006) Recent developments in superhydrophobic surfaces and their relevance to marine fouling: A review. *Biofouling* 22:339–360.
18. Meyer B (2003) Approaches to prevention, removal and killing of biofilms. *Int Biodeter Biodegr* 51:249–253.
19. Banerjee I, Pangule RC, Kane RS (2011) Antifouling coatings: Recent developments in the design of surfaces that prevent fouling by proteins, bacteria, and marine organisms. *Adv Mater*.
20. Zhao L, Chu PK, Zhang Y, Wu Z (2009) Antibacterial coatings on titanium implants. *J Biomed Mater Res B Appl Biomater* 91:470–480.
21. Autumn K, et al. (2002) Evidence for van der Waals adhesion in gecko setae. *Proc Natl Acad Sci USA* 99:12252–12256.
22. Jiang SY, Cao ZQ (2010) Ultralow-fouling, functionalizable, and hydrolyzable zwitterionic materials and their derivatives for biological applications. *Adv Mater* 22:920–932.
23. Callow JA, Callow ME (2011) Trends in the development of environmentally friendly fouling-resistant marine coatings. *Nat Commun* 2:244.
24. Harris JM (1992) *Poly(ethylene glycol) Chemistry: Biotechnical and Biomedical Applications* (Plenum Press, New York).
25. Park KD, et al. (1998) Bacterial adhesion on PEG modified polyurethane surfaces. *Biomaterials* 19:851–859.
26. Prime KL, Whitesides GM (1991) Self-assembled organic monolayers: Model systems for studying adsorption of proteins at surfaces. *Science* 252:1164–1167.
27. Lee BP, Messersmith P, Israelachvili J, Waite J (2011) Mussel-inspired adhesives and coatings. *Ann Rev Mater Res* 41:99–132.
28. Brzozowska AM, de Keizer A, Detrembleur C, Cohen Stuart MA, Norde W (2010) Grafted ionomer complexes and their effect on protein adsorption on silica and polysulfone surfaces. *Colloid Polym Sci* 288:1621–1632.
29. Voets IK, et al. (2008) Internal structure of a thin film of mixed polymeric micelles on a solid/liquid interface. *J Phys Chem B* 112:6937–6945.
30. Fadeeva E, et al. (2011) Bacterial retention on superhydrophobic titanium surfaces fabricated by femtosecond laser ablation. *Langmuir* 27:3012–3019.
31. Bos R, Mei H, Gold J, Busscher H (2000) Retention of bacteria on a substratum surface with micro patterned hydrophobicity. *Fems Microbiol Lett* 189:311–315.
32. Gristina A (1987) Biomaterial-centered infection: Microbial adhesion versus tissue integration. *Science* 237:1588–1595.
33. Neu T (1996) Significance of bacterial surface-active compounds in interaction of bacteria with interfaces. *Microbiol Mol Biol R* 60:151–166.
34. Poetes R, Holtzmann K, Franze K, Steiner U (2010) Metastable underwater superhydrophobicity. *Phys Rev Lett* 105:166104.
35. Hall-Stoodley L, Costerton JW, Stoodley P (2004) Bacterial biofilms: From the natural environment to infectious diseases. *Nat Rev Microbiol* 2:95–108.
36. Trevors J (1987) Silver resistance and accumulation in bacteria. *Enzyme Microb Tech* 9:331–333.
37. Costerton J, Stewart P, Greenberg E (1999) Bacterial biofilms: A common cause of persistent infections. *Science* 284:1318–1322.
38. Bohn HF, Federle W (2004) Insect aquaplaning: Nepenthes pitcher plants capture prey with the peristome, a fully wettable water-lubricated anisotropic surface. *Proc Natl Acad Sci USA* 101:14138–14143.
39. Wong TS, et al. (2011) Bioinspired self-repairing slippery surfaces with pressure-stable omniphobicity. *Nature* 477:443–447.
40. Boswell PG, Bühlmann P (2005) Fluorous bulk membranes for potentiometric sensors with wide selectivity ranges: Observation of exceptionally strong ion pair formation. *J Am Chem Soc* 127:8958–8959.
41. Zhao H, Ismail K, Weber SG (2004) How fluororous is poly (2, 2-bis (trifluoromethyl)-4, 5-difluoro-1, 3-dioxide-co-tetrafluoroethylene)(Teflon AF)? *J Am Chem Soc* 126:13184–13185.
42. Zhang H, Hussam A, Weber SG (2010) Properties and transport behavior of perfluorotriptylamine (FC-70)-doped amorphous teflon AF 2400 films. *J Am Chem Soc* 132:17867–17879.
43. Zhao H, et al. (2005) Transport of organic solutes through amorphous teflon AF films. *J Am Chem Soc* 127:15112–15119.
44. Khoo X, et al. (2010) *Staphylococcus aureus* resistance on titanium coated with multivalent PEGylated-peptides. *Biomaterials* 31:9285–9292.
45. Picknett RG, Bexon R (1977) Evaporation of sessile or pendant drops in still air. *J Colloid Interf Sci* 61:336–350.
46. Deegan RD, et al. (1997) Capillary flow as the cause of ring stains from dried liquid drops. *Nature* 389:827–829.
47. Jung JY, Kim YW, Yoo JY, Koo J, Kang YT (2010) Forces acting on a single particle in an evaporating sessile droplet on a hydrophilic surface. *Anal Chem* 82:784–788.
48. Wong TS, Chen TH, Shen XY, Ho CM (2011) Nanochromatography driven by the coffee ring effect. *Anal Chem* 83:1871–1873.
49. Tsai YP (2005) Impact of flow velocity on the dynamic behaviour of biofilm bacteria. *Biofouling* 21:267–277.
50. Purevdorj B, Costerton J, Stoodley P (2002) Influence of hydrodynamics and cell signaling on the structure and behavior of *Pseudomonas aeruginosa* biofilms. *Appl and Environ Microb* 68:4457–4464.
51. O'Toole GA, Kolter R (1998) Initiation of biofilm formation in *Pseudomonas fluorescens* WCS365 proceeds via multiple, convergent signalling pathways: A genetic analysis. *Mol Microbiol* 28:449–461.
52. Ozawa H, Kumon H, Yokoyama T, Watanabe T, Chancellor MB (1998) Development of noninvasive velocity flow video urodynamics using Doppler sonography. Part II: Clinical application in bladder outlet obstruction. *J Urol* 160:1792–1796.
53. GABE IT, et al. (1969) Measurement of instantaneous blood flow velocity and pressure in conscious man with a catheter-tip velocity probe. *Circulation* 40:603–614.
54. Lowe KC (2003) Engineering blood: Synthetic substitutes from fluorinated compounds. *Tissue Eng* 9:389–399.
55. O'Toole GA, Kolter R (1998) Flagellar and twitching motility are necessary for *Pseudomonas aeruginosa* biofilm development. *Mol Microbiol* 30:295–304.
56. Gibiansky ML, et al. (2010) Bacteria use type IV pili to walk upright and detach from surfaces. *Science* 330:197.
57. Wilking C, Weitz D (2010) Bacteria in confined spaces. *B Am Phys Soc* 55.
58. Marcoux PR, et al. (2010) Micro-confinement of bacteria into w/o emulsion droplets for rapid detection and enumeration. *Colloids Surf A Physicochem Eng Aspects* 377:54–62.
59. Clausell-Tormos J, et al. (2008) Droplet-based microfluidic platforms for the encapsulation and screening of mammalian cells and multicellular organisms. *Chem Biol* 15:427–437.
60. Shim J-u, et al. (2009) Simultaneous determination of gene expression and enzymatic activity in individual bacterial cells in microdroplet compartments. *J Am Chem Soc* 131:15251–15256.
61. Kintses B, van Vliet LD, Devenish SRA, Hoffelder F (2010) Microfluidic droplets: New integrated workflows for biological experiments. *Curr Opin Chem Biol* 14:548–555.
62. Rosenberg M (1991) Basic and applied aspects of microbial adhesion at the hydrocarbon: Water interface. *Crit Rev Microbiol* 18:159–173.
63. Desbief S, et al. (2009) Superhydrophobic aluminum surfaces by deposition of micelles of fluorinated block copolymers. *Langmuir* 26:2057–2067.
64. Guo Z, Zhou F, Hao J, Liu W (2005) Stable Biomimetic super-hydrophobic engineering materials. *J Am Chem Soc* 127:15670–15671.
65. Liu L, Zhao J, Zhang Y, Zhao F, Zhang Y (2011) Fabrication of superhydrophobic surface by hierarchical growth of lotus-leaf-like boehmite on aluminum foil. *J Colloid Interf Sci* 358:277–283.
66. Sugawara M (1998) *Plasma Etching: Fundamentals and Applications* (Oxford University Press, New York).